



CK2 and GSK3 phosphorylation on S29 controls wild-type ATXN3 nuclear uptake

V. Pastori^a, E. Sangalli^a, P. Coccetti^a, C. Pozzi^a, S. Nonnis^b, G. Tedeschi^b, P. Fusi^{a,*}

^a Dipartimento di Biotecnologie e Bioscienze, Università di Milano-Bicocca, P.za della Scienza 2, 20126 Milan, Italy

^b D.I.P.A.V. (Dipartimento di Patologia Animale, Igiene e Sanità Pubblica Veterinaria), Università degli Studi di Milano, via Celoria 10, 20133, Milan, Italy

ARTICLE INFO

Article history:

Received 28 July 2009

Received in revised form 9 March 2010

Accepted 14 March 2010

Available online 27 March 2010

Keywords:

ATXN3

Phosphorylation

CK2

GSK3

Subcellular localization

Mass spectrometry

ABSTRACT

In the present work we show that murine ATXN3 (ATXN3Q6) nuclear uptake is promoted by phosphorylation on serine 29, a highly conserved residue inside the Josephin domain. Both casein kinase 2 (CK2) and glycogen synthase kinase 3 (GSK3) are able to carry out phosphorylation on this residue. S29 phosphorylation was initially assessed *in vitro* on purified ATXN3Q6, and subsequently confirmed in transfected COS-7 cells, by MS analysis. Site-directed mutagenesis of S29 to an alanine was shown to strongly reduce nuclear uptake, in COS-7 transiently transfected cells overexpressing ATXN3Q6, while substitution with phospho-mimic aspartic acid restored the wild-type phenotype. Finally, treatment with CK2 and GSK3 inhibitors prevented S29 phosphorylation and strongly inhibited nuclear uptake, showing that both kinases are involved in ATXN3Q6 subcellular sorting. Although other authors have previously addressed this issue, we show for the first time that ATXN3 is phosphorylated inside the Josephin domain and that S29 phosphorylation is involved in nuclear uptake of ATXN3.

© 2010 Elsevier B.V. All rights reserved.

1. Introduction

Ataxin-3 (ATXN3), the protein involved in SCA3 (Spinocerebellar Ataxia type 3), is a ubiquitously expressed protein [1–3], possessing a conserved N-terminal region, the Josephin domain, and a less conserved, unstructured C-terminus containing the poly-Q stretch [4–6]. The structure of the Josephin domain has been determined by NMR [7,8].

Many hypothesis have been formulated as regards ATXN3 function [9–13]. On the whole, recent data suggest a role for ATXN3 in proteasome mediated protein degradation, as a deubiquitinating enzyme which regulates flow through the ERAD (ER Associated Degradation) [7,14].

ATXN3 is mostly cytosolic, although it also localizes in the nucleus [15,16]. Nuclear localization is particularly relevant to SCA3 pathogenesis, in that pathologically expanded ATXN3 gives rise to nuclear aggregates. Different authors [13,17–20] presented evidence suggesting a model of the disease in which the full-length pathological protein is recruited into aggregates by “toxic” poly-Q containing fragments. In our laboratory we observed that purified ATXN3 underwent slow autolytic fragmentation [21] and subsequently showed that pathological ATXN3 was less proteolyzed than its normal counterpart [22]. Besides, some authors showed that ATXN3 is the target of caspase 1 [13], while others demonstrated that ATXN3 is cleaved by calpains [20,23].

The role of phosphorylation in SCA3 pathogenesis has not yet been thoroughly investigated. Tait and coworkers have shown the presence, in ATXN3 primary structure, of two putative casein kinase (CK2) phosphorylation sites [15]. Other authors [24] have shown that ATXN3 interacts with CK2. More recently Mueller and coworkers [25] showed that ATXN3 phosphorylation by CK2 on S340 and S352 promotes ATXN3 nuclear uptake. Protein kinase CK2 is a highly conserved, ubiquitously expressed Ser/Thr kinase, extremely abundant in the brain. This pleiotropic enzyme is involved in the control of various cellular processes [26], amongst which neural development [27]. Moreover, the catalytic α -subunit of CK2 is an inhibitor of the neuronal kinase Cdk5 [28]. Fei and coworkers [29] showed that ATXN3 is also phosphorylated by glycogen synthase kinase 3 β (GSK 3 β), a Ser/Thr kinase, particularly abundant in the central nervous system [30] that plays a key role in a number of cellular processes [31].

In this work we find that a murine form (ATXN3Q6) [32,33], is phosphorylated by CK2 and GSK3 on serine 29, a highly conserved residue inside the Josephin domain. We also show that phosphorylation at this residue controls nuclear uptake of ATXN3, a key event in SCA3 pathogenesis.

2. Materials and Methods

2.1. Constructs

cDNA coding for murine ATXN3Q6, previously subcloned in our laboratory into plasmid *pGEX-6P-1*, was cut with *Bam*HI and *Xho*I restriction enzymes and subcloned into plasmid *pcDNA3X(+)*HA (Invitrogen UK Ltd. Paisley, England). Subsequently, ATXN3 coding

* Corresponding author. Tel.: +39 0264483405; fax: +39 0264483409.
E-mail address: paola.fusi@unimib.it (P. Fusi).

cDNA, tagged with an HA epitope at the N-terminal, was retrieved by PCR from *pcDNA3X(+)*HA and subcloned into plasmid *pcDNA3.1/myc-His*, digested with the same enzymes, in frame with a *c-myc* epitope; the STOP codon was eliminated by site-directed mutagenesis.

S29A and S29D mutants were obtained by PCR using Quik-Change Site directed Mutagenesis Kit (Stratagene La Jolla, CA USA), according to the manufacturer's instructions. The correct insertion of cDNAs in expression vectors and the presence of the mutations were verified by automated sequencing using vector oligonucleotide primers (T7 and BGH).

All constructs in *pcDNA3.1/myc-His*, carrying N-terminal HA and C-terminal *c-myc* epitopes, were hosted and amplified in *E. coli* strain DH5 α , while protein expression was achieved after transient transfection of COS-7 cells or SHSY-5Y cells. Cultures were carried out in 94 mm plates in DMEM containing 10% fetal bovine serum (FBS), 100 U/ml penicillin, 100 μ g/ml streptomycin and 4 mM glutamine (COS-7 cells) or in F12 and DMEM containing 10% fetal bovine serum (FBS), 100 U/ml penicillin, 100 μ g/ml streptomycin and 4 mM glutamine (SHSY-5Y cells). Cells were subsequently transiently transfected with FuGENE6 (Roche Diagnostics Mannheim, Germany), according to the manufacturer's instructions. To inhibit CK2 and GSK3, COS-7 cells were incubated for 24 hours at 37 °C with either 5 or 10 μ M CK2 inhibitor (TBB, Sigma St. Louis, Mo, USA) and/or with 10 μ M GSK3 inhibitor (SB216763, Sigma St. Louis, Mo, USA). 24 h after transfection, cells were harvested and tested for subcellular localization of exogenous ATXN3 by blotting and detection with *c-myc* antibody. Cell viability was assessed through MTT test (Sigma St. Louis, Mo, USA), performed according to the manufacturer's instructions.

2.2. Cell fractionation

24 h after transfection, COS-7 cells (6×10^5 cells/plate, cultured in 94 mm plates) or SHSY-5Y cells (1×10^6 cells/plate, cultured in 94 mm plates) were harvested and resuspended in 10 mM (Na)PO $_4$, 100 mM NaCl, pH 7.4, 0.5% NP-40, supplemented with protease inhibitors (Roche Diagnostics Mannheim, Germany). After incubating 40 min on ice, nuclei were pelleted by centrifugation at $4000 \times g$ for 15 min at 4 °C. The supernatant, was centrifuged at $15,000 \times g$ for 30 min at 4 °C, yielding the cytosolic fraction. Nuclei were resuspended in 50 mM HEPES pH 7.9, 0.75 mM MgCl $_2$, 0.5 mM EDTA, 0.5 M NaCl, 12.5% glycerol, 5 mM DTT and protease inhibitors. After incubating 1 h on ice nuclei were centrifuged at $15,000 \times g$ for 30 min at 4 °C: the supernatant represented the nuclear fraction.

2.3. Immunoprecipitation

1000 μ g total protein extract, obtained from ATXN3Q6 over-expressing COS-7 cells, was incubated overnight at 4 °C with an anti-ATXN-3 polyclonal antibody, (2 μ g of Z46 antibody (Primm Cambridge, MA USA). The total extract was subsequently incubated with Protein A-Sepharose TM-CL-4B (Amersham GE Healthcare, Uppsala, Sweden) for 2 h at 4 °C. After incubation the resin was washed 3 times with NP40 buffer (50 mM Tris pH 7.5, 150 mM NaCl, 15 mM MgCl $_2$ and 1% NP40) and ataxin-3 was eluted by boiling in SDS buffer.

2.4. SDS-PAGE and western-blot analysis

SDS-PAGE and Western-blot were carried out by standard procedures. PVDF ImmobilonTM P (Millipore Billerica, MA USA) membranes were blocked for 1 h in PBS, containing either 5% (w/v) dried milk (for anti-*c-myc* antibody) or in 5% (w/v) bovine serum albumin (BSA) (Sigma St. Louis, Mo, USA) (for anti-fibrillarin and anti-Phosphoglycerate kinase (PGK) antibodies). Membranes were subsequently probed overnight in PBS 1% dried milk, with anti-*c-myc*

mouse monoclonal antibody (1:1000) (Santa Cruz Biotechnology Inc. Santa Cruz, CA. USA). Control incubations with anti-fibrillarin (1:5000) (Encor Biotechnology Gainesville, FL, USA) and with 22C5 anti-PGK (1:1000) (Molecular Probes, Invitrogen UK Ltd. Paisley, England) mouse monoclonal antibodies were also carried out overnight in PBS, containing 1% (w/v) BSA, 0.1% (v/v) Tween20 and 1% (w/v) BSA respectively. Membranes, probed with mouse antibodies, were incubated for 1 h with an anti-mouse horseradish peroxidase-conjugated IgG (1:3000) (Calbiochem Darmstadt, Germany) in PBS, containing 0.1% (v/v) Tween20 and 1% (w/v) dried milk. Detection of antibody binding was carried out with ECL (Amersham GE Healthcare, Uppsala, Sweden), according to the manufacturer's instructions.

Protein levels were quantified by densitometry of scanned not saturated X-ray films using the NIH Image-based software Scion Image (Scion Corporation). Quantification data are a mean of three independent experiments; bands intensities were normalized on fibrillarin and PGK controls. Statistical analysis was performed using t-Student test, results significance was indicated with $p < 0.05$.

2.5. Acid silver stain

SDS-PAGE was fixed for 1 h in 40% Ethanol, 10% acid acetic and for 2 days in 5% ethanol, 5% acid acetic; the gel was subsequently washed 3 times for 20 min in 30% ethanol and incubated for 1 min in 0.8 mM sodium tiosulfate. The gel was then incubated in 11.8 mM silver nitrate, 0.02% formaldehyde for 20 min and subsequently washed twice with water for 20 sec and developed with 556 mM sodium carbonate, 0.02% formaldehyde, 0.02 mM sodium tiosulfate. Developing was stopped with 50% ethanol, 12% acid acetic; the gel was washed with water for 10 min and conserved at 4 °C in 1% acid acetic.

2.6. Immunofluorescence and confocal analysis

COS-7 cells were plated onto coverslips (2.5×10^4 cells/coverslip) and grown for 24 h before transfection. Cells were transfected overnight with FuGENE6 (Roche Diagnostics Mannheim, Germany); 24 h after transfection, cells were fixed for 20 min in 3% (w/v) paraformaldehyde in PBS and quenched for 30 min with 50 mM NH $_4$ Cl in PBS. Permeabilization was carried out by incubating the cells in the presence of 0.3% (w/v) saponin in PBS (7 min for 3 times). Cells were then doubly stained with anti-*c-myc* mouse monoclonal antibody (Santa Cruz Biotechnology Inc. Santa Cruz, CA USA) and anti-HA rabbit polyclonal antibody (Sigma St. Louis, Mo USA). After extensive washes, cells were incubated with donkey anti-mouse Cy3 conjugated antibody and donkey anti-rabbit Cy2 conjugated antibody. All antibodies were from Jackson ImmunoResearch Laboratories (West Grove, PA USA). Incubations and washes were carried out at room temperature in PBS, 0.3% (w/v) saponin. Cells were finally incubated for 15 min with the nuclear marker TO-PRO-3 iodide (Molecular Probes, Invitrogen UK Ltd Paisley, England). Confocal microscopy was performed using a Leica Mod. TCS-SP2 (Leica Microsystem). Image processing was performed with Leica Confocal Software (LCS) and Adobe Photoshop Software. Confocal microscopy images were collected under the same conditions in order to compare fluorescence intensities among different images. About 120 cells were examined in each image and 6 images were analyzed for each experiment; the nuclear region was circumscribed and its mean fluorescence intensity was evaluated. Statistical analysis was performed using t-Student test, results significance was indicated with $p < 0.05$.

2.7. Purification from E.coli

ATXN3Q6-encoding cDNA, cloned into plasmid *pGEX-6P-1*, was used to transform *E. coli* strain BL21 codon plus RIL, to express ATXN3

as a GST-fusion protein. Cells were grown at 37 °C in LB-ampicillin medium and induced at A_{600} 0.8, for 3 h with 50 μ M IPTG. In order to obtain crude extracts, cells were resuspended in lysis buffer (10 mM potassium phosphate, pH 7.2, 150 mM NaCl, 1 mM phenylmethanesulfonyl fluoride, 5 mM DTT, 100 mM $MgCl_2$) plus 1 mg/ml lysozyme and incubated for 1 h at 4 °C. Cell suspension was then frozen at -80 °C for 20 min and thawed; DNase I (0.15 mg/g of cells, wet weight) and 1% Triton X-100 were added, and the sample further incubated for 30 min at room temperature. After centrifugation for 30 min at 18,000 \times g, the supernatant was incubated with Glutathione Sepharose 4B resin (1 ml/g of cells, wet weight) (GE Healthcare, Uppsala, Sweden) for 40 min at 4 °C; the sample was subsequently loaded onto the column. After washing with 10 volumes of PBS (10 mM potassium phosphate, pH 7.2, 150 mM NaCl) and equilibration with 10 volumes of cold Cleavage Buffer (50 mM Tris-HCl, pH 7.0, 150 mM NaCl, 1 mM EDTA, 1 mM DTT), ATXN3 was cleaved from fusion partner by overnight incubation at 4 °C with PreScission Protease (80 U/ml resin) (GE Healthcare, Uppsala, Sweden). Purified ATXN3 was eluted with 10 ml of Cleavage buffer. Protein concentration was assayed through Coomassie brilliant blue G-250 from Pierce (Pierce Biotechnology, Rockford, IL), using bovine plasma immunoglobulin as a standard protein.

2.8. *In vitro* phosphorylation by CK2

ATXN3Q6 purified from *E. coli* was dialyzed for 3 h at 4 °C against 50 mM Tris pH 8, 150 mM NaCl, 10 mM $MgCl_2$, with a 14 kD cut-off membrane. ATXN3Q6 (40 μ g) was then incubated for 30 min at 30 °C, under shaking, with 1 μ g (200 U) CK2 (BIOMOL international Plymouth Meeting, PA USA) in the presence of 1 mM ATP. The sample was then subjected to MALDI-TOF analysis. If needed, phosphorylation was checked using [γ - 32 P]ATP, as previously reported [34].

2.9. *In vitro* phosphorylation by GSK3

ATXN3Q6 purified from *E. coli* was dialyzed for 3 h at 4 °C in GSK3 buffer (25 mM MOPS pH 7.2, 12.5 mM β -glycerophosphate, 5 mM EGTA, 2 mM EDTA, 25 mM $MgCl_2$, 0.25 mM DTT, 50 ng/ μ l BSA) with a 14 kD cut-off membrane. ATXN3Q6 (40 μ g) was then incubated with 1 μ g (100U) GSK3 (BIOMOL international Plymouth Meeting, PA. USA) and ATP 100 μ M at 30 °C for 30 min. The sample was then subjected to analysis.

2.10. Mass spectrometry analysis

ATXN3Q6, phosphorylated *in vitro* by either CK2 or GSK3 as described above, was subjected to reduction and alkylation in solution by iodoacetamide and incubated with GluC endoproteases (1:25 enzyme/protein, w/w) overnight at 37 °C. Following acidification, the peptide mixture was loaded onto a MALDI plate using ZipTip C18 (Millipore, Bedford, MA-USA) with a matrix of α -ciano-4-hydroxycinnamic acid. The same procedure was applied for the analysis of ATXN3Q6 in transfected cells. In the latter case the protein, separated by SDS-PAGE, was subjected to *in situ* digestion with GluC endoprotease (1:10 enzyme/protein, w/w) and peptide extraction with 40% CH_3CN in 0.1% TFA before loading onto the MALDI plate. Mass spectrometry analysis was carried out on a Bruker Daltonics Reflex IV instrument (Bruker Daltonics, Milano, Italy) equipped with a nitrogen laser, operating in positive and negative linear mode. Each spectrum was accumulated for at least 200 laser shots and Bruker peptide calibration standards were used for calibration.

MS/MS analysis was carried out on a MALDI TOF/TOF Autoflex III (Bruker Daltonics, Milano, Italy). Data were acquired and processed using Biotoools software (Bruker Daltonics, Milano, Italy).

3. Results

3.1. ATXN3 is phosphorylated *in vitro* by Casein Kinase II

A bioinformatic analysis, performed through NetPhos 2.0, NetPhosK 1.0 and ScanProsite servers available at www.expasy.ch, as well as Phosidia server available at Phosidia.com, showed the presence, along ATXN3 aminoacidic sequence, of a series of phosphorylation consensus sites for several kinases. However, within the Josephin domain, the only structured part of the protein, only one residue (S29) was predicted by all four servers to be phosphorylated with a high score. This site appears to be highly conserved in vertebrates, from fish to mammals, as shown in Fig. 1a. According to ScanProsite, NetPhos 2.0 and Phosidia servers, S29 is phosphorylated by CK2, despite the presence of a proline at the C-terminal side of the phosphorylated residue; moreover phosphorylation by GSK3 is also predicted at S29 by NetPhosK 1.0 server. As shown in Fig. 1a, another highly conserved consensus site for CK2 is S236, a residue located upstream of the poly-Q stretch, but outside the Josephin domain, which is also predicted to be phosphorylated by CK2 by all servers. S256, another highly conserved phosphorylation site, predicted to be phosphorylated by GSK3 by NetPhos 2.0 and Phosidia servers, was already demonstrated to be phosphorylated by this kinase [29]. Other consensus sites were found in the C-terminal unstructured domain: a cluster of five phosphorylation sites predicted to be phosphorylated either by CK2 or by GSK3 (S268, T271, S272, S273, S277) and the two serines already demonstrated to be phosphorylated by CK2 by Mueller and coworkers (S329 and S341 in murine ATXN3, corresponding to S340 and S352 respectively in human ATXN3) [25]. However, most of these sites (as well as others such as S321 and T344) are not predicted to be phosphorylated by all four servers, nor are they highly conserved, as shown in Fig. 1a.

In order to ascertain whether ATXN3 can be phosphorylated by CK2, purified recombinant murine ATXN3Q6, obtained as previously reported [33], was subjected to *in vitro* phosphorylation by CK2. Autoradiography (Fig. 1b) showed that ATXN3 is actually phosphorylated by this kinase, confirming that sites phosphorylatable by CK2 are present in this protein, as previously reported [25,29]. Lower molecular mass bands are also seen, representing ATXN3 proteolytic fragments, whose characterization was described in a previous work [22]. Since none of the existing studies on ATXN3 phosphorylation had been carried out through mass spectrometry, we decided to investigate ATXN3 phosphorylation through a proteomic approach. The study of the role of CK2 phosphorylation at S29 and S236 appeared of particular interest, since these are the most conserved CK2 phosphorylation sites, the C-terminal domain being more divergent, and because no previous study had investigated phosphorylation of the N-terminus.

3.2. ATXN3 is phosphorylated *in vitro* by CK2 and GSK3 on S29

In order to assess which of the predicted CK2 and/or GSK3 phosphorylatable residues are actually phosphorylated, recombinant ATXN3 was subjected to *in vitro* phosphorylation by either CK2 or GSK3, digestion with GluC and mass spectrometry analysis. Operating in the linear mode, upon incubation of wild-type ATXN3 with either CK2 or GSK3, it was possible to detect peaks corresponding to monophosphorylated peptides containing S29 (Fig. 2). A list of the phosphorylated peptides identified through mass spectrometry is reported in Fig. 2a. The peak at 3002.13 m/z was also analyzed by MS/MS TOF-TOF analysis unequivocally confirming the phosphorylation of ATXN3 on S29 residue (data not shown). Upon phosphatase treatment the corresponding non-phosphorylated peaks were detected (data not shown). Fig. 2b reports three of the spectra relative to the peptides, obtained after phosphorylation with CK2: peak at 2172.32 m/z corresponds to the phosphorylated peptide 27-

44 ($^{27}\text{YFSPVELSSIAHQLEDEE}^{44}$, calculated average mass 2172.97), peak at 3002.13 m/z corresponds to the phosphorylated peptide 8–32 ($^8\text{KQEGSLCAQHCLNLLQGEYFSPVE}^{32}$, calculated monoisotopic mass 3001.35) and peak at 3516.00 m/z corresponds to the phosphorylated peptide 3–32 ($^3\text{SIFHEKQEGSLCAQHCLNLLQGEYFSPVE}^{32}$, calculated monoisotopic mass 3516.64). Moreover, mass spectrometric analysis of the protein fingerprint allowed to detect only peptides containing unmodified S236, showing that this residue is not phosphorylated in such conditions.

Besides the modification in the Josephin domain, phosphorylation at serine residues in the C-terminal portion of the molecule was also observed: S268, S272, S273, S277, T271, S329 and S341, were all found to be phosphorylated by CK2; S268, S272, S273 and S277 were also found to be phosphorylated by GSK3 (data not shown). These findings are in accordance with previous data reported by Mueller and coworkers [25], who described the phosphorylation of human ATXN3 at S340 and S352, corresponding to murine ATXN3 S329 and S341 respectively.

Taken together, our results provide evidence that ATXN3 is phosphorylated *in vitro* on residue S29 by CK2 and GSK3 and suggest a direct role of these kinases in *in vivo* phosphorylation of ATXN3 within the Josephin domain.

3.3. ATXN3 is phosphorylated in transfected COS-7 cells

COS-7 cells overexpressing ATXN3Q6 were collected 24 h after transfection; the recombinant protein was immunoprecipitated from crude extracts with anti-ATXN3Q6 polyclonal Z46 antibody and subsequently loaded onto SDS-PAGE. Bands were detected through acid silver staining and subjected to *in situ* digestion with Glu-C endoprotease. Mass spectrometry analysis of the protein expressed in transfected cells unequivocally confirmed that ATXN3Q6 is phosphorylated at S29, since it was possible to detect phosphopeptides containing S29 upon fingerprint mass analysis, as reported in Table 1 (phosphopeptide $^{27}\text{YFSPVE}^{32}$, calculated monoisotopic mass 821.34, experimental mass 821.98, and phosphopeptide $^{27}\text{YFSPVELSSIAHQLEDEE}^{44}$, calculated monoisotopic mass 2172.97, experimental mass 2173.02).

3.4. ATXN3Q6S29A is less efficiently translocated to the nucleus than the wild-type

With the aim of investigating the role of phosphorylation on S29, this residue was substituted with an alanine, through site-directed mutagenesis performed with Quik Change Mutagenesis Kit (Stratagene La Jolla, CA USA). COS-7 cells were transiently transfected with plasmid *pcDNA3.1/myc-His*, expressing either wild-type ATXN3Q6 or ATXN3Q6S29A carrying an HA epitope at the N-terminus and a *c-myc* epitope at the C-terminus. Cells were harvested 24 h after transfection and cytosolic and nuclear fractions were analysed by Western blotting, probed with a monoclonal anti-*c-myc* antibody. Results are shown in Fig. 3a: the band corresponding to wild-type ATXN3Q6 was found equally distributed between the cytoplasm and the nucleus. On the contrary, the band corresponding to S29A mutant was found much less abundant in the nuclear fraction, being about 25% of the intensity of the corresponding cytosolic band, as shown by densitometric analysis (Fig. 3c); statistical analysis confirmed the existence of a significant difference between nuclear and cytosolic S29A mutant ($p < 0.05$); no differences were found between nuclear and cytosolic wild-type ATXN3 ($p = 0.52$). This suggests that S29 phosphorylation

promotes ATXN3 nuclear uptake. Confocal microscopy confirmed these results: as seen in Fig. 4a wild-type ATXN3Q6 fluorescence, both red (due to Cy3 conjugated anti-*c-myc* antibody) and green (due to Cy2 conjugated anti-HA antibody), was evenly distributed inside the cells. On the other hand, S29A mutant fluorescence was found to be much weaker inside the nucleus than in the cytoplasm. The overlay with the blue fluorescence emission of the nuclear marker confirmed that wild-type ATXN3 is found also inside the nucleus, while S29A mutant is found predominantly in the cytosol. Quantitative analysis of fluorescent emission allowed to assess that S29A mutant fluorescence in the nuclear region amounted to about 30% of wild-type ATXN3 fluorescence in the same area (Fig. 4b); statistically significant differences were found between wild-type ATXN3 and S29A mutant ($p < 0.05$).

In order to confirm the role of S29 phosphorylation on ATXN3 nuclear uptake, this residue was substituted with an aspartic acid, thus mimicking the presence of the phosphate negative charge. After ATXN3Q6S29D transient expression in COS-7 cells, cytoplasmic and nuclear fractions were analysed by Western blotting. Results, shown in Fig. 3b, showed that S29D behaved exactly like the wild-type, being equally distributed in the nucleus and the cytoplasm. Consistently, a uniform fluorescence distribution inside the cells was detected in confocal microscopy experiments, as shown in Fig. 4a, the overlay showing colocalization with the nuclear marker. Quantitative fluorescence analysis confirmed that S29D fluorescence in the nuclear region did not remarkably differ from that of wild-type ATXN3Q6 (Fig. 4b); statistical analysis yielded a p value 0.53, confirming the absence of any statistically significant differences between wild-type ATXN3 and S29D mutant.

Moreover the same percentage of cells showing the described subcellular localization was found in all samples considered, as shown in the last column of Fig. 4a. Cell viability, assayed through MTT test, showed a 30% reduction for S29A mutant, when compared to both wild-type protein and S29D mutant; statistical analysis of three different experiments yielded a p value < 0.05 for the comparison between wild-type ATXN3 and S29A mutant, while a p value of 0.21 was found when comparing wild-type ATXN3 with S29D mutant.

The previously observed [22] 42 kDa fragment, produced by proteolytic cleavage at S29, was found almost exclusively in the cytosolic fractions and appeared to be more evident in S29A mutant than in the wild-type protein and in S29D mutant.

In order to rule out the possibility that the observed phenotype of S29A mutant might be confined to COS-7 cells, human neuroblastoma SHSY-5Y cells were also transfected with plasmid *pcDNA3.1/myc-His*, expressing either wild-type ATXN3Q6 or ATXN3Q6S29A carrying an HA epitope at the N-terminus and a *c-myc* epitope at the C-terminus. Cytosolic and nuclear fractions, obtained from harvested cells 24 h after transfection, were analysed by Western blotting, probed with a monoclonal anti-*c-myc* antibody. Results, reported in Fig. 3d, show the absence of S29A in the nuclear fraction, in accordance with what observed in COS-7 cells.

3.5. CK2 and GSK3 inhibitors demonstrate that both kinases act on S29 in COS-7 transfected cells

COS-7 cells expressing either ATXN3Q6 or ATXN3Q6S29D were grown in the presence of CK2 inhibitor TBB (tetrabromobenzotriazole) and GSK3 inhibitor SB216763. Inhibitors were added to growth media either separately or in combination. Western-blots of nuclear and cytosolic fractions, probed with anti-*c-myc* antibody, are shown in

Fig. 1. *In vitro* CK2 phosphorylation of ATXN3. (a) T-Coffee multiple sequence alignment of ataxins-3: *Anas platyrhynchos* (duck; ABX10879), *Danio rerio* (zebrafish; AAY28605), *Canis lupus* (dog; XP537352), *Xenopus laevis* (african clawed frog; NP001016389), *Bos taurus* (domestic cow; AAI46167), *Ornithorhynchus anatinus* (platypus; XP001507271), *Homo sapiens* (man; BAI46626), *Mus musculus* (mouse; NP083981), *Macaca rhesus* (macaque; XP001116022), *Branchiostoma lanceolatum* (amphioxus XP002610252); conserved serines are marked. (b) *In vitro* phosphorylation of purified recombinant murine ATXN3Q6 (arrow); an *E. coli* crude extract subjected to the same purification procedure (see Materials and Methods) was used as a control.

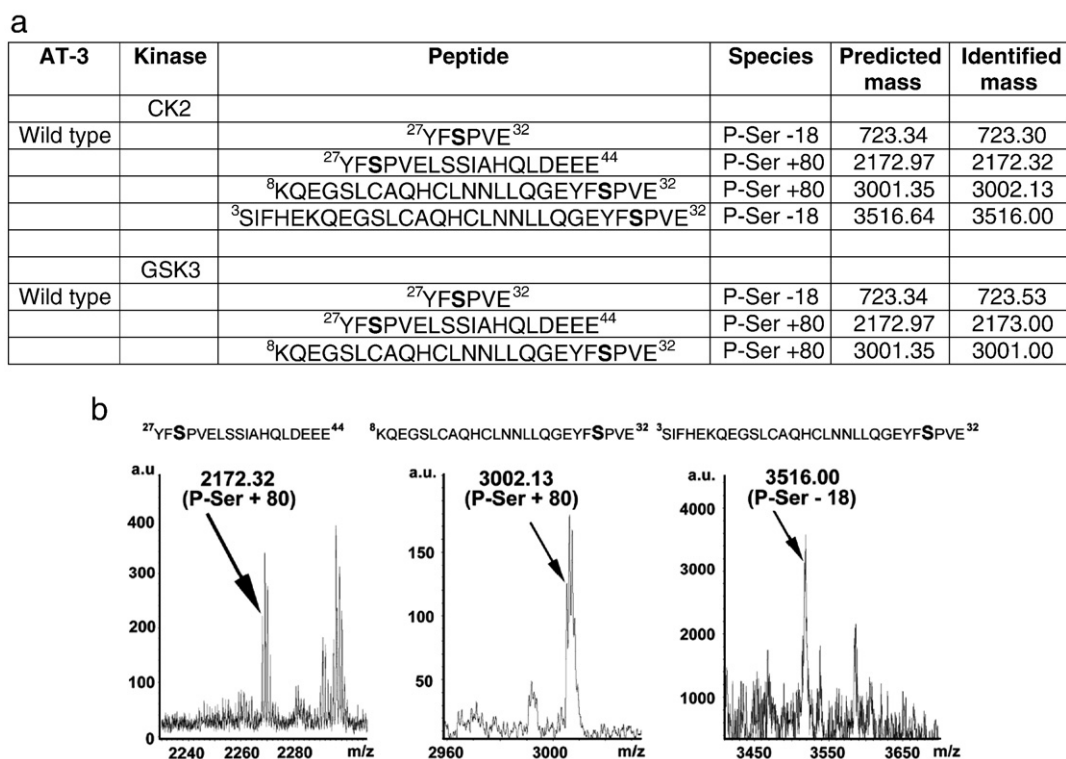


Fig. 2. ATXN3 is phosphorylated on Ser 29 by CK2 and GSK3. (a) 8 μ g of ATXN3 was phosphorylated in vitro either by CK2 or GSK3. Samples were denatured in 8 M urea and subjected to reduction and alkylation in solution by iodoacetamide. After dilution and incubation with GluC endoproteinas (1:25 enzyme/protein, w/w) overnight at 37 °C, samples were analysed by Mass analysis (as described in the experimental section). The presence of the phosphate group results in an increase in mass of 80 units or in a decrease of 18 units due to the loss of the phosphate and a water molecule. (b) Peak at 2172.32 m/z corresponds to the CK2 phosphorylated peptide 27–44 (²⁷YFSPVELSSIAHQLDEEE⁴⁴, calculated average mass 2172.97), peak at 3002.13 m/z corresponds to the CK2 phosphorylated peptide 8–32 (⁸KQEGSLCAQHCLNNLLQGEYFSPVE³², calculated monoisotopic mass 3001.35) and peak at 3516.00 m/z corresponds to the CK2 phosphorylated peptide 3–32 (³SIFHEKQEGSLCAQHCLNNLLQGEYFSPVE³², calculated monoisotopic mass 3516.64) are indicated. Data are representative of one of three experiments.

Fig. 5. When the culture medium was supplemented with TBB alone, as shown in Fig. 5a, both wild-type ATXN3Q6 and S29D mutant were found evenly distributed between the cytosol and the nucleus, suggesting that TBB could not prevent S29 phosphorylation even at 10 μ M concentration. The same happened when only GSK3 inhibitor SB216763 was administered at 10 μ M concentration, as shown in Fig. 5b.

However, when both inhibitors were added to culture medium, nuclear translocation of wild-type ATXN3Q6 appeared to be reduced, a behaviour closely mirroring that of S29A mutant (see Fig. 5c); on the contrary, S29D mutant appeared to be uniformly distributed between nucleus and cytosol. Intensities of ATXN3 bands in total extracts were found to be similar, showing that the mutation did not affect ATXN3 expression levels. These data were confirmed by densitometric analysis, reported in Fig. 5d, showing that, when both inhibitors were administered, about 50% of the intensity of the corresponding cytosolic band of wild-type ATXN3 was found inside the nucleus, while S29D mutant was equally distributed between the two cellular compartments; the statistically significant difference in nuclear and

cytosolic localization of ATXN3 in the presence of the inhibitors was confirmed by a p value <0.05. Mass spectrometry analysis, performed on acid silver stained gels after ATXN3Q6 immunoprecipitation from COS-7 cells cultured in the presence of both TBB and SB216763, allowed to detect a peptide containing unmodified S29, (²⁷YFSPVELSSIAHQLDEEE⁴⁴, calculated monoisotopic mass 2092.97, experimental mass 2092.78), showing that this residue is not phosphorylated when both CK2 and GSK3 inhibitors are present.

On the whole these data clearly show that CK2 and GSK3 can concur in the phosphorylation of S29, promoting ATXN3 nuclear uptake.

4. Discussion

Phosphorylation is well known to play a role in a number of neurodegenerative diseases, notably in amyloid fibers formation. Nonaka and coworkers [35] have shown that α -synuclein is phosphorylated on Ser 129 and that this is crucial in mediating both protein neurotoxicity and inclusion formation; other authors have shown that huntingtin is phosphorylated by Cdk5 [36]. Phosphorylation has also been reported to protect presenilin-2 from caspase cleavage [37]. Amongst ataxias, SCA14 is caused by mutations on residues which are normally phosphorylated: unphosphorylated proteins do not fold correctly and aggregate [38]; ATXN1, the protein responsible for Sca1 has been demonstrated to be phosphorylated by Akt at S776; this phosphorylation creates a binding site for 14-3-3, increasing ATXN1 stabilization and accumulation and hence leading to pathogenesis [39,40]. Amongst the kinases involved in neurodegenerative diseases, CK2 and GSK3 are particularly interesting. In neuronal cells there appears to be a myriad of CK2 substrates that have clear implications in neural development, neuritogenesis,

Table 1

ATXN3 is phosphorylated on Ser 29 in transfected cells. Cell homogenate was separated by SDS-PAGE and ATXN3Q6 was subjected to reduction, alkylation and in situ digestion with GluC endoproteinase (1:10 enzyme/protein, w/w). Upon peptide extraction with 40% CH₃CN in 0.1% TFA, the peptide mixture was analyzed by mass spectrometry (as described in Materials and Methods).

ATX3	Peptide	Species	Predicted mass	Identified mass
Wild type	²⁷ YFSPVE ³²	P-Ser +80	821.34	821.98
	²⁷ YFSPVELSSIAHQLDEEE ⁴⁴	P-Ser +80	2172.97	2173.02

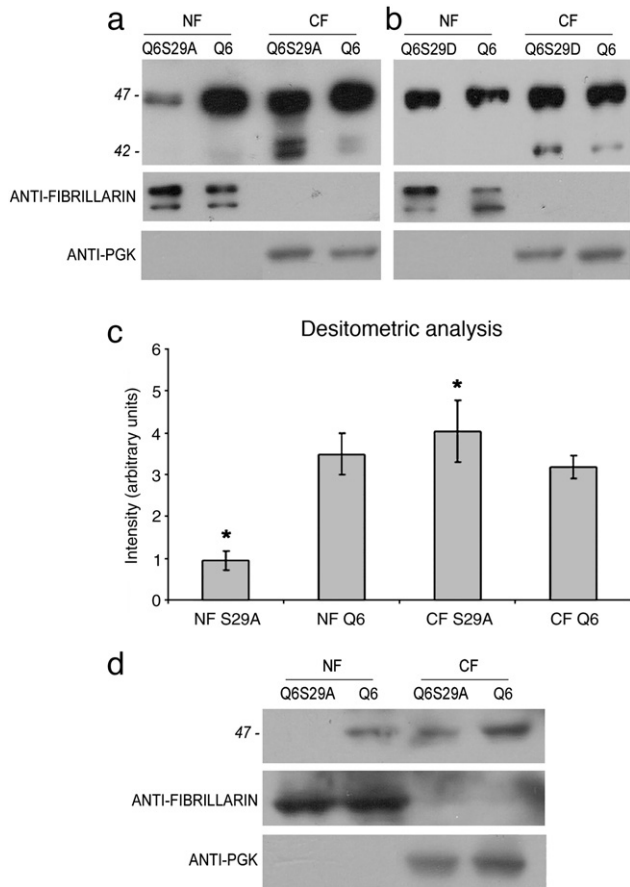


Fig. 3. Western-blot analysis of ataxins-3 in COS-7 and SHSY-5Y cells. *c-myc* tagged full-length ATXN3Q6 (a, b) and its mutants ATXN3Q6S29A (a) and ATXN3Q6S29D (b) were expressed in COS-7 cells. Western-blot of cytosolic and nuclear fractions were probed with a monoclonal anti-*c-myc* antibody. Cytosolic and nuclear fractions controls were performed with anti-fibrillarin and anti-PGK antibodies. (c) Densitometric analysis performed with NIH Image-based software Scion Image (Scion Corporation) on blot reported in panel a. Bands intensities were normalized on fibrillarin and PGK controls. Data represent mean \pm SD of three independent experiments; significant differences were found between nuclear and cytosolic S29A mutant (* $p < 0.05$); no differences were found between nuclear and cytosolic wild-type ATXN3 ($p = 0.52$) (d) *c-myc* tagged full-length ATXN3Q6 and its mutant ATXN3Q6S29A were expressed in SHSY-5Y cells. Western-blot of cytosolic and nuclear fractions were probed with a monoclonal anti-*c-myc* antibody. Cytosolic and nuclear fractions controls were performed with anti-fibrillarin and anti-PGK antibodies.

synaptic transmission and plasticity [27]. On the other hand, of the two isoforms of GSK3 which are found in mammals, GSK3 β and GSK3 α [41], GSK3 β is particularly abundant in the central nervous system [30] and has been found to be involved in Alzheimer disease pathogenesis [42].

Some authors already addressed the issue of ATXN3 phosphorylation [15,24,25,29], however, their studies were conducted mainly through pull-down assays and coimmunoprecipitations.

In this work, we investigated for the first time the role of ATXN3 phosphorylation through a proteomic approach. Amongst the different putative phosphorylation consensus sites which are found along ATXN3 sequence, we found that S29, the only phosphorylatable site within the Josephin domain, can be phosphorylated *in vitro* by both CK2 and GSK3. Phosphorylation on S29 was subsequently confirmed in transfected COS-7 cells overexpressing ATXN3Q6 and was found to be prevented by the addition of CK2 and GSK3 inhibitors. On the contrary, S236, another highly conserved phosphorylation site, was found to be unphosphorylated in mass spectrometry analysis. Moreover, our data confirmed phosphorylation at C-terminal sites already described by other authors, such as S256 [29] and S329 and S341, corresponding to S340 and S352 respectively in human ATXN3

[25]. It is worth mentioning that Serine 29 is recognized, by prediction methods, as part of a consensus sequence for both CK2 and GSK3, although the presence of a proline nearby is known to prevent phosphorylation by CK2 in some instances; experimental data allowed to confirm this prediction.

Our decision to focus on S29 phosphorylation is motivated by the fact that this residue is highly conserved in vertebrates; moreover, it is the only putatively phosphorylated site within the Josephin domain and, according to the NMR determined structure [8] is fully exposed to the solvent and presumably easily accessible. On the other hand, we did not focus on consensus sites located in the C-terminal domain, since they appear to be less conserved and had already been studied by other authors.

In order to assess whether phosphorylation at S29 could regulate ATXN3 subcellular localization, we substituted S29 with an alanine, through site-directed mutagenesis. Results showed that mutation to alanine strongly reduced nuclear uptake. The fact that, upon substituting S29 with an aspartic acid, the wild-type phenotype is restored, shows that the reduction of nuclear uptake is due to the lack of the negative phosphate charge and not to the aminoacid substitution. The site of proteolytic cleavage seems to be unaffected by the lack of phosphorylation; however S29A mutant seems to be cleaved at S29 to a higher extent than both wild-type and S29D mutant, suggesting that phosphorylation at this level might hamper proteolytic cleavage; the double band which is seen in correspondence of S29A 42 kDa fragment is also present in wild-type ATXN3 and is probably an artifact. More work will be necessary to elucidate the nature and role of the so far unknown protease involved in the cleavage.

Mass spectrometry analysis also showed beyond any doubt that ATXN3 is phosphorylated in transfected cells and this strongly suggests that phosphorylation takes place also *in vivo*. Moreover, the fact that CK2 and GSK3 concur in phosphorylating S29 points to the importance of ATXN3 nuclear translocation. Results obtained with both inhibitors suggest that no other kinases are involved in this process.

All our experiments have been performed on murine ATXN3, carrying only six glutamines and sharing a high similarity with normal human ATXN3; as stated before [22], the choice of this protein is justified by the effort to avoid aggregate formation, which can be artificially induced by the unnatural raising in concentration which takes place inside transfected cells, since the aggregation process follows a second order kinetic [33]. The presence of only six glutamines in murine ATXN3, makes the event rather unlikely. Moreover we already showed that human ATXN3Q26 behaves exactly like murine ATXN3Q6 when expressed at low levels in transfected cells, as regards subcellular sorting and proteolytic fragmentation [22].

Our data show a strong reduction in nuclear uptake, which is nevertheless not completely abolished. The possibility that this event is controlled by more than one factor is very likely. In a recent paper, Mueller et al. identified CK2 phosphorylation on S340 and S352, two residues which are found downstream of poly-Q, as essential for nuclear translocation [25]; although, as mentioned above, we did not focus on phosphorylation at these residues, our data are definitely not in contrast with those of Mueller and coworkers. Since S340 and S352 are both found inside UIM3, whose presence in ATXN3 structure depends on alternative splicing, phosphorylation at S29 may well be an additional factor promoting nuclear uptake, a process which seems essential for ATXN3 function. In addition, ATXN3 nuclear uptake does not seem to be completely suppressed in Mueller and coworkers experiments [25], neither upon S340/S352 mutagenesis to alanine nor upon addition of CK2 inhibitors. Last but not least, the fact that when S29 is substituted with an alanine, a 30% decrease in cell viability is observed, suggests that nuclear uptake is an important process for ATXN3 functionality, possibly in relation to its function as a transcriptional repressor [9,43], and is finely controlled by more

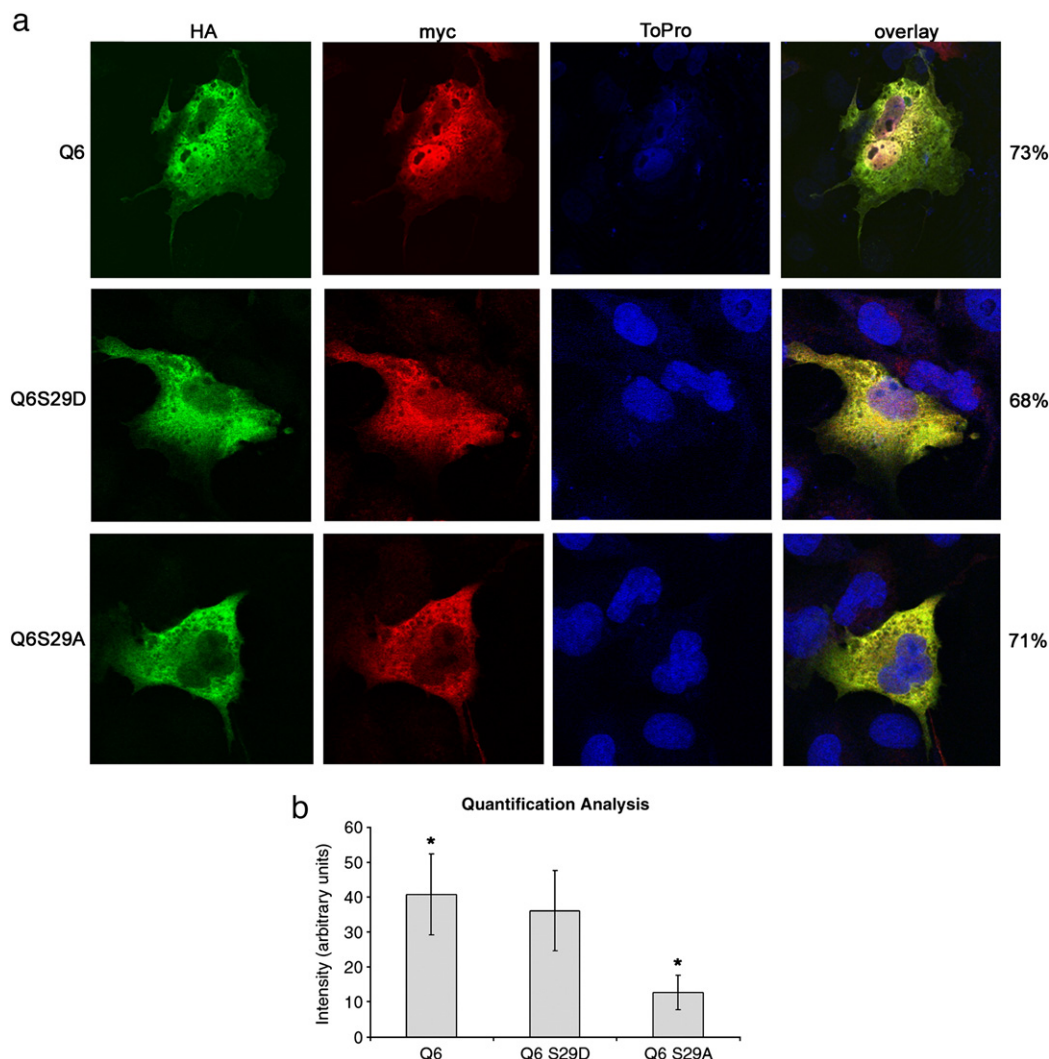


Fig. 4. Confocal microscopy analysis of ATXN3 subcellular localization. (a) COS-7 cells were transfected with cDNAs coding for ATXN3Q6, or ATXN3Q6S29A and ATXN3Q6S29D mutants. To investigate sub-cellular localization of ATXN3, cells were fixed in PFA and probed with mouse monoclonal anti-c-myc (red), rabbit monoclonal anti-HA antibodies (green) and the nuclear marker TO-PRO-3 iodide (blue). Last column reports percentage of observed phenotypes (b) Quantification analysis of fluorescence intensities in the nuclear region of cells overexpressing ATXN3Q6, ATXN3Q6S29A or ATXN3Q6S29D. Data represent mean \pm SD of three independent experiments; significant differences were found between wild-type ATXN3 and S29A mutant (* $p < 0.05$); no differences were found between wild-type ATXN3 and S29D mutant ($p = 0.53$).

than one factor. In contrast to Mueller and coworkers, a recent paper [44] showed that CK2 inhibitors are not effective in preventing ATXN3 nuclear localization upon heat-shock; this is well in accordance with our data showing that only simultaneous inhibition of both CK2 and GSK3 can prevent ATXN3 nuclear uptake. These authors also showed that S111, which is found inside a Polo-like kinase phosphorylation site, is involved in ATXN3 nuclear uptake following heat-shock; we propose that this residue be involved in nuclear uptake promoted by heat-shock or oxidative stress, while phosphorylation at S29, S340 and S352 could regulate normal ATXN3 trafficking between the nucleus and the cytoplasm. This is strongly supported by the fact that, in Reina and coworkers experiments, S111 mutation to alanine decreases ATXN3 nuclear localization but does not suppress it.

Whether a putative NLS, which is found in ATXN3 primary sequence, is essential for ATXN3 nuclear translocation is still controversial: in a previous work [22] we showed that a truncated mutant lacking this sequence was only slightly less efficiently translocated into the nucleus; Mueller and coworkers, as well as Reina and coauthors, recently confirmed that NLS mutation has no effect on ATXN3 subcellular distribution. On the other hand other

authors [45] showed, through a yeast nuclear import assay, that ATXN3 NLS is functional and essential for nuclear uptake.

Nuclear translocation of ATXN3 is also of the utmost importance for SCA3 pathogenesis, since amyloid aggregates are found primarily inside the nucleus. Although a growing amount of data suggest that mitochondrial damage is also involved in SCA3 pathogenesis [46–48], the presence of nuclear aggregates is a hallmark of many neurodegenerative diseases and impairment of nuclear functions is very likely to induce cell death. Our data strongly suggest that inhibiting S29 phosphorylation, strongly reduces ATXN3 nuclear uptake. This in turn leads to the key question of how S29 phosphorylation is involved in SCA3 pathogenesis. In a previous work [22] we suggested that a toxic poly-Q containing fragment is produced from incomplete proteolysis of pathological human ATXN3Q72, which can trigger aggregation of pathological undegraded ATXN3, upon reaching a critical concentration inside mitochondria and the nucleus. Recently, Hubener et al. [49] showed that in transgenic mice nuclear aggregation of pathological ATXN3 occurs even when an expanded ATXN3 carrying a NES is coexpressed and demonstrated that double transgenic mice, expressing both normal and pathological ATXN3 show the same disease

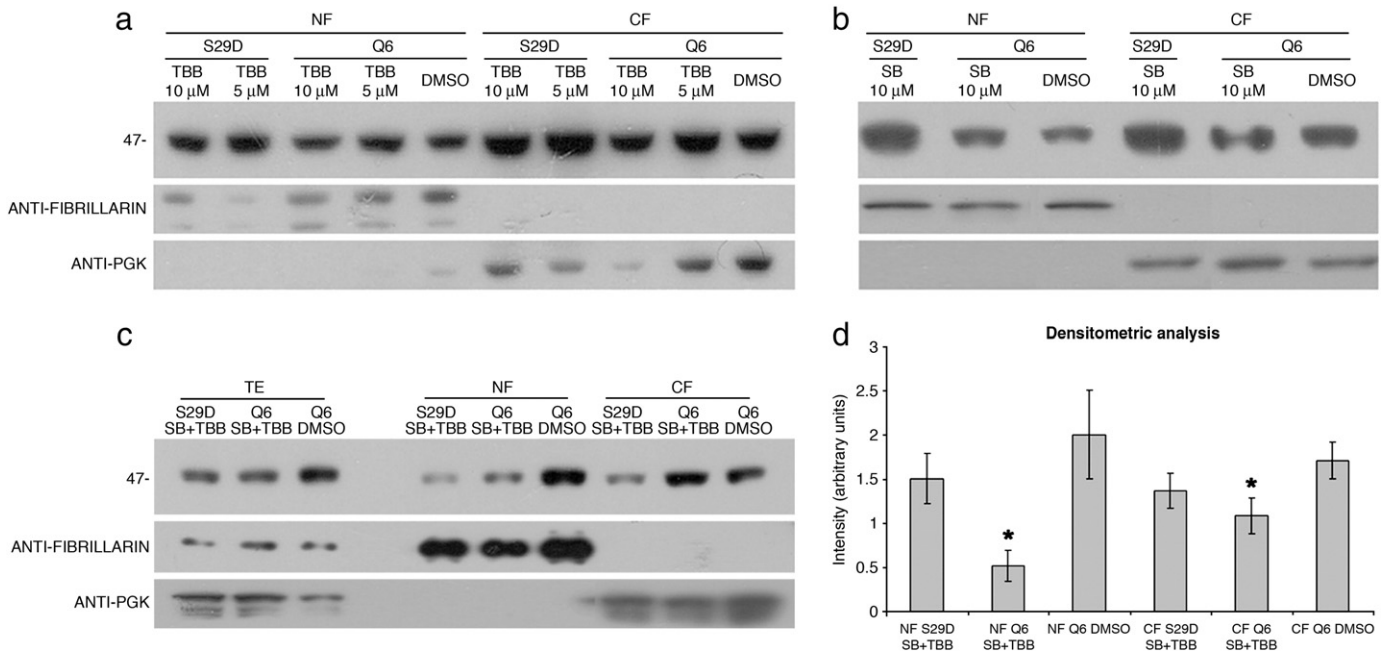


Fig. 5. Western-blot analysis of COS-7 cells treated with kinase inhibitors. (a) *c-myc* tagged full-length ATXN3Q6 and its mutant ATXN3Q6S29D were expressed in COS-7 cells treated with TBB 5 or 10 μ M (CK2 inhibitor) or with DMSO, as a control. (b) *c-myc* tagged full-length ATXN3Q6 and its mutant ATXN3Q6S29D were expressed in COS-7 cells treated with SB 216763 10 μ M (GSK3 inhibitor) or with DMSO, as a control. (c) *c-myc* tagged full-length ATXN3Q6 and its mutant ATXN3Q6S29D were expressed in COS-7 cells treated with both TBB 10 μ M (CK2 inhibitor) and SB 216763 10 μ M (GSK3 inhibitor) or with DMSO, as a control. (d) Densitometric analysis performed with NIH Image-based software Scion Image (Scion Corporation) on blot reported in panel c. Bands intensities were normalized on fibrillarin and PGK controls. Data represent mean \pm SD of three independent experiments; significant differences were found between nuclear and cytosolic wild-type ATXN3 in the presence of CK2 and GSK3 inhibitors (* $p < 0.05$); no differences were found between nuclear and cytosolic S29D mutant in the presence of CK2 and GSK3 inhibitors ($p > 0.5$) (a, b, c). Western-blot of total extracts, cytosolic fraction and nuclear fraction were probed with a monoclonal anti-*c-myc* antibody. Cytosolic and nuclear fractions controls were performed with anti-fibrillarin and anti-PGK antibodies.

progression, as transgenic mice expressing only the pathological proteins; this is consistent with the idea that aggregation is a concentration process and could also be explained by the already proposed hypothesis of expanded polyQ stretching giving rise to membrane channels. Moreover another recent work [50] showed that the C-terminus of Hsp70-interacting protein (CHIP) suppresses ATXN3Q70 neurotoxicity in transgenic mice, preventing the formation of toxic microaggregates. Ubiquitinylation by either E4B or CHIP is essential to target misfolded ATXN3 to the proteasome [10,24]. Data of different authors [24,25] have shown that pathological ATXN3 is also a substrate of CK2, suggesting that phosphorylation may target pathological ATXN3 to the nucleus, where it will readily form aggregates, escaping ubiquitinylation and targeting to proteasomal degradation. Further work will be undertaken in order to understand the role of CK2 and GSK3 in SCA3 pathogenesis.

Acknowledgements

The authors would like to thank Dr Anna Maria Villa (Dipartimento di Biotecnologie e Bioscienze, Università di Milano-Bicocca, Milan, Italy) for technical support in immunofluorescence experiments.

References

- [1] H.L. Paulson, S.S. Das, P.B. Crino, M.K. Perez, S.C. Patel, D. Gotsdiner, K.H. Fischbeck, R.N. Pittman, Machado-Joseph disease gene product is a cytoplasmic protein widely expressed in brain, *Ann. Neurol.* 41 (1997) 453–462.
- [2] Y. Trottier, G. Cancel, I. An-Gourfinkel, Y. Lutz, C. Weber, A. Brice, E. Hirsch, J.L. Mandel, Heterogeneous intracellular localization and expression of ataxin-3, *Neurobiol. Dis.* 5 (1998) 335–347.
- [3] A.E. Bevilacqua, P.J. Loll, An expanded glutamine repeat destabilizes native ataxin-3 structure and mediates formation of parallel β -fibrils, *Proc. Natl. Acad. Sci. U. S. A.* 98 (2001) 11955–11960.
- [4] M. Albrecht, D. Hoffmann, B.O. Evert, I. Schmitt, U. Wullner, T. Lengauer, Structural modeling of ataxin-3 reveals distant homology to adaptins, *Proteins* 50 (2003) 355–370.
- [5] L. Masino, V. Musi, R.P. Menon, P. Fusi, G. Kelly, T.A. Frenkiel, Y. Trottier, A. Pastore, Domain architecture of the polyglutamine protein ataxin-3: a globular domain followed by a flexible tail, *FEBS Lett.* 549 (2003) 21–25.
- [6] M. Albrecht, M. Golatta, U. Wullner, T. Lengauer, Structural and functional analysis of ataxin-2 and ataxin-3, *Eur. J. Biochem.* 271 (2004) 3155–3170.
- [7] Y. Mao, F. Senic-Matuglia, P.P. Di Fiore, S. Polo, M.E. Hodsdon, P. De Camilli, Deubiquitinating function of ataxin-3: insights from the solution structure of the Josephin domain, *Proc. Natl. Acad. Sci. U. S. A.* 102 (2005) 12700–12705.
- [8] G. Nicastro, R.P. Menon, L. Masino, P.P. Knowles, N.Q. McDonald, A. Pastore, The solution structure of the Josephin domain of ataxin-3: structural determinants for molecular recognition, *Proc. Natl. Acad. Sci. U. S. A.* 102 (2005) 10493–10498.
- [9] F. Li, T. Macfarlan, R.N. Pittman, D. Chakravarti, Ataxin-3 is a histone-binding protein with two independent transcriptional corepressor activities, *J. Biol. Chem.* 277 (2002) 45004–45012.
- [10] M. Matsumoto, M. Yada, S. Hatakeyama, H. Ishimoto, T. Tanimura, S. Tsuji, A. Kakizuka, M. Kitagawa, K.I. Nakayama, Molecular clearance of ataxin-3 is regulated by a mammalian E4, *EMBO J.* 23 (2004) 659–669.
- [11] H. Scheel, S. Tomiuk, K. Hofmann, Elucidation of ataxin-3 and ataxin-7 function by integrative bioinformatics, *Hum. Mol. Genet.* 12 (2003) 2845–2852.
- [12] B. Burnett, F. Li, R.N. Pittman, The polyglutamine neurodegenerative protein ataxin-3 binds polyubiquitylated proteins and has ubiquitin protease activity, *Hum. Mol. Genet.* 12 (2003) 3195–3205.
- [13] S.J. Berke, F.A. Schmied, E.R. Brunt, L.M. Ellerby, H.L. Paulson, Caspase-mediated proteolysis of the polyglutamine disease protein ataxin-3, *J. Neurochem.* 89 (2004) 908–918.
- [14] X. Zhong, R.N. Pittman, Ataxin-3 binds VCP/p97 and regulates retrotranslocation of ERAD substrates, *Hum. Mol. Genet.* 15 (2006) 2409–2420.
- [15] D. Tait, M. Riccio, A. Sittler, E. Scherzinger, S. Santi, A. Ognibene, N.M. Maraldi, H. Lehrach, E.E. Wanker, Ataxin-3 is transported into the nucleus and associates with the nuclear matrix, *Hum. Mol. Genet.* 7 (1998) 991–997.
- [16] M.K. Perez, H.L. Paulson, R.N. Pittman, Ataxin-3 with an altered conformation that exposes the polyglutamine domain is associated with the nuclear matrix, *Hum. Mol. Genet.* 8 (1999) 2377–2385.
- [17] C.L. Wellington, L.M. Ellerby, A.S. Hackam, R.L. Margolis, M.A. Trifiro, R. Singaraja, K. McCutcheon, G.S. Salvesen, S.S. Propp, M. Bromm, K.J. Rowland, T. Zhang, D. Rasper, S. Roy, N. Thornberry, L. Pinsky, A. Kakizuka, C.A. Ross, D.W. Nicholson, D. E. Bredesen, M.R. Hayden, Caspase cleavage of gene products associated with triplet expansion disorders generates truncated fragments containing the polyglutamine tract, *J. Biol. Chem.* 273 (1998) 9158–9167.
- [18] H.L. Paulson, Protein fate in neurodegenerative proteinopathies: polyglutamine diseases join the (mis)fold, *Am. J. Hum. Genet.* 64 (1999) 339–345.
- [19] D. Goti, S.M. Katzen, J. Mez, N. Kurtis, J. Kiluk, L. Ben-Haim, N.A. Jenkins, N.G. Copeland, A. Kakizuka, A.H. Shoup, C.A. Ross, P.R. Mouton, V. Colomer, A mutant ataxin-3 putative-cleavage fragment in brains of Machado-Joseph disease

- patients and transgenic mice is cytotoxic above a critical concentration, *J. Neurosci.* 24 (2004) 10266–10279.
- [20] A. Haacke, S.A. Broadley, R. Boteva, N. Tzvetkov, F.U. Hartl, P. Breuer, Proteolytic cleavage of polyglutamine-expanded ataxin-3 is critical for aggregation and sequestration of non-expanded ataxin-3, *Hum. Mol. Genet.* 15 (2006) 555–568.
 - [21] P.L. Mauri, M. Riva, D. Ambu, A. De Palma, F. Secundo, L. Benazzi, M. Valtorta, P. Tortora, P. Fusi, Ataxin-3 is subject to autolytic cleavage, *FEBS J.* 273 (2006) 4277–4286.
 - [22] C. Pozzi, M. Valtorta, G. Tedeschi, E. Galbusera, V. Pastori, A. Bigi, S. Nonnis, E. Grassi, P. Fusi, Study of subcellular localization and proteolysis of ataxin-3, *Neurobiol. Dis.* 30 (2008) 190–200.
 - [23] A. Haacke, F.U. Hartl, P. Breuer, Calpain inhibition is sufficient to suppress aggregation of polyglutamine-expanded ataxin-3, *J. Biol. Chem.* 282 (2007) 18851–18856.
 - [24] R.S. Tao, E.K. Fei, Z. Ying, H.F. Wang, G.H. Wang, Casein kinase 2 interacts with and phosphorylates ataxin-3, *Neurosci. Bull.* 24 (2008) 271–277.
 - [25] T. Mueller, P. Breuer, I. Schmitt, J. Walter, B.O. Evert, U. Wullner, CK2-dependent phosphorylation determines cellular localization and stability of ataxin-3, *Hum. Mol. Genet.* 18 (2009) 3334–3343.
 - [26] H.G. Lee, G. Perry, P.J. Moreira, M.R. Garrett, Q. Liu, X. Zhu, A. Takeda, A. Nunomura, M.A. Smith, Tau phosphorylation in Alzheimer's disease: pathogen or protector? *Trends Mol. Med.* 11 (2005) 164–169.
 - [27] L. Chen, M.B. Feany, Alpha-synuclein phosphorylation controls neurotoxicity and inclusion formation in a *Drosophila* model of Parkinson disease, *Nat. Neurosci.* 8 (2005) 657–663.
 - [28] A.C. Lim, Z. Hou, C.P. Goh, R.Z. Qi, Protein kinase CK2 is an inhibitor of the neuronal Cdk5 kinase, *J. Biol. Chem.* 279 (2004) 46668–46673.
 - [29] E. Fei, N. Jia, T. Zhang, X. Ma, H. Wang, C. Liu, W. Zhang, L. Ding, N. Nukina, G. Wang, Phosphorylation of ataxin-3 by glycogen synthase kinase 3 β at serine 256 regulates the aggregation of ataxin-3, *Biochem. Biophys. Res. Commun.* 357 (2007) 487–492.
 - [30] M.D. Kaytor, H.T. Orr, The GSK3 β signaling cascade and neurodegenerative disease, *Curr. Opin. Neurobiol.* 12 (2002) 275–278.
 - [31] R.S. Jope, G.V. Johnson, The glamour and gloom of glycogen synthase kinase-3, *Trends Biochem. Sci.* 29 (2004) 95–102.
 - [32] S. Marchal, E. Shehi, M.C. Harricane, P. Fusi, F. Heitz, P. Tortora, R. Lange, Structural instability and fibrillar aggregation of non-expanded human ataxin-3 revealed under high pressure and temperature, *J. Biol. Chem.* 278 (2003) 31554–31563.
 - [33] E. Shehi, P. Fusi, F. Secundo, S. Pozzuolo, A. Bairati, P. Tortora, Temperature-dependent, irreversible formation of amyloid fibrils by a soluble human ataxin-3 carrying a moderately expanded polyglutamine stretch (Q36), *Biochemistry* 42 (2003) 14626–14632.
 - [34] P. Coccetti, R.L. Rossi, F. Sternieri, D. Porro, G.L. Russo, A. di Fonzo, F. Magni, M. Vanoni, L. Alberghina, Mutations of the CK2 phosphorylation site of Sic1 affect cell size and S-Cdk kinase activity in *Saccharomyces cerevisiae*, *Mol. Microbiol.* 51 (2004) 447–460.
 - [35] T. Nonaka, T. Iwatsubo, M. Hasegawa, Ubiquitination of alpha-synuclein, *Biochemistry* 44 (2005) 361–368.
 - [36] S. Luo, C. Vacher, J.E. Davies, D.C. Rubinshtein, Cdk5 phosphorylation of huntingtin reduces its cleavage by caspases: implications for mutant huntingtin toxicity, *J. Cell Biol.* 169 (2005) 647–656.
 - [37] J. Walter, A. Schindzielorz, J. Grunberg, C. Haass, Phosphorylation of presenilin-2 regulates its cleavage by caspases and retards progression of apoptosis, *Proc. Natl. Acad. Sci. U. S. A.* 96 (1999) 1391–1396.
 - [38] T. Seki, N. Adachi, Y. Ono, H. Mochizuki, K. Hiramoto, T. Amano, H. Matsubayashi, M. Matsumoto, H. Kawakami, N. Saito, N. Sakai, Mutant protein kinase C γ found in spinocerebellar ataxia type 14 is susceptible to aggregation and causes cell death, *J. Biol. Chem.* 280 (2005) 29096–29106.
 - [39] H.K. Chen, P. Fernandez-Funez, S.F. Acevedo, Y.C. Lam, M.D. Kaytor, M.H. Fernandez, A. Aitken, E.M. Skoulakis, H.T. Orr, J. Botas, H.Y. Zoghbi, Interaction of Akt-phosphorylated ataxin-1 with 14-3-3 mediates neurodegeneration in spinocerebellar ataxia type 1, *Cell* 113 (2003) 457–468.
 - [40] E.S. Emamian, M.D. Kaytor, L.A. Duvick, T. Zu, S.K. Tousey, H.Y. Zoghbi, H.B. Clark, H.T. Orr, Serine 776 of ataxin-1 is critical for polyglutamine-induced disease in SCA1 transgenic mice, *Neuron* 38 (2003) 375–387.
 - [41] J.R. Woodgett, Molecular cloning and expression of glycogen synthase kinase-3/ β factor A, *EMBO J.* 9 (1990) 2431–2438.
 - [42] J.J. Lucas, F. Hernandez, P. Gomez-Ramos, M.A. Moran, R. Hen, J. Avila, Decreased nuclear beta-catenin, tau hyperphosphorylation and neurodegeneration in GSK-3 β conditional transgenic mice, *EMBO J.* 20 (2001) 27–39.
 - [43] B.O. Evert, J. Araujo, A.M. Vieira-Saecker, R.A. de Vos, S. Harendza, T. Klockgether, U. Wullner, Ataxin-3 represses transcription via chromatin binding, interaction with histone deacetylase 3, and histone deacetylation, *J. Neurosci.* 26 (2006) 11474–11486.
 - [44] C.P. Reina, X. Zhong, R.N. Pittman, Proteotoxic stress increases nuclear localization of ataxin-3, *Hum. Mol. Genet.* 19 (2010) 235–249.
 - [45] S. Macedo-Ribeiro, L. Cortes, P. Maciel, A.L. Carvalho, Nucleocytoplasmic shuttling activity of ataxin-3, *PLoS One* 4 (2009) e5834.
 - [46] H.F. Tsai, H.J. Tsai, M. Hsieh, Full-length expanded ataxin-3 enhances mitochondrial-mediated cell death and decreases Bcl-2 expression in human neuroblastoma cells, *Biochem. Biophys. Res. Commun.* 324 (2004) 1274–1282.
 - [47] A.H. Chou, T.H. Yeh, Y.L. Kuo, Y.C. Kao, M.J. Jou, C.Y. Hsu, S.R. Tsai, A. Kakizuka, H.L. Wang, Polyglutamine-expanded ataxin-3 activates mitochondrial apoptotic pathway by upregulating Bax and downregulating Bcl-xL, *Neurobiol. Dis.* 21 (2006) 333–345.
 - [48] Y.C. Yu, C.L. Kuo, W.L. Cheng, C.S. Liu, M. Hsieh, Decreased antioxidant enzyme activity and increased mitochondrial DNA damage in cellular models of Machado-Joseph disease, *J. Neurosci. Res.* 87 (2009) 1884–1891.
 - [49] J. Hubener, O. Riess, Polyglutamine-induced neurodegeneration in SCA3 is not mitigated by non-expanded ataxin-3: Conclusions from double-transgenic mouse models, *Neurobiol. Dis.* 38 (1) (2010) 116–124.
 - [50] A.J. Williams, T.M. Knutson, V.F. Colomer Gould, H.L. Paulson, In vivo suppression of polyglutamine neurotoxicity by C-terminus of Hsp70-interacting protein (CHIP) supports an aggregation model of pathogenesis, *Neurobiol. Dis.* 33 (2009) 342–353.